AIP Applied Physics Letters

Atomic layer deposition of Al-incorporated Zn(O,S) thin films with tunable electrical properties

Helen Hejin Park, Ashwin Jayaraman, Rachel Heasley, Chuanxi Yang, Lauren Hartle, Ravin Mankad, Richard Haight, David B. Mitzi, Oki Gunawan, and Roy G. Gordon

Citation: Applied Physics Letters **105**, 202101 (2014); doi: 10.1063/1.4901899
View online: http://dx.doi.org/10.1063/1.4901899
View Table of Contents: http://scitation.aip.org/content/aip/journal/apl/105/20?ver=pdfcov
Published by the AIP Publishing

Articles you may be interested in

Atomic layer deposition of Zn(O,S) thin films with tunable electrical properties by oxygen annealing
Appl. Phys. Lett. **102**, 132110 (2013); 10.1063/1.4800928

Atomic layer deposition of Al-doped ZnO thin films
J. Vac. Sci. Technol. A **31**, 01A109 (2013); 10.1116/1.4757764

Low temperature atomic layer deposited Al-doped ZnO thin films and associated semiconducting properties
J. Vac. Sci. Technol. B **30**, 031210 (2012); 10.1116/1.4710519

Growth morphology and electrical/optical properties of Al-doped ZnO thin films grown by atomic layer deposition
J. Vac. Sci. Technol. A **30**, 021202 (2012); 10.1116/1.3687939

Effective atomic layer deposition procedure for Al-dopant distribution in ZnO thin films
J. Vac. Sci. Technol. A **28**, 1111 (2010); 10.1116/1.3460905

This article is copyrighted as indicated in the article. Reuse of AIP content is subject to the terms at: http://scitation.aip.org/termsconditions. Downloaded to IP: 66.31.20.16 On: Wed, 19 Nov 2014 17:47:27

APPLIED PHYSICS LETTERS **105**, 202101 (2014)

Atomic layer deposition of Al-incorporated Zn(O,S) thin films with tunable electrical properties

Helen Hejin Park,[1] Ashwin Jayaraman,[1] Rachel Heasley,[1] Chuanxi Yang,[1] Lauren Hartle,[1] Ravin Mankad,[2] Richard Haight,[2] David B. Mitzi,[2,3] Oki Gunawan,[2] and Roy G. Gordon[1,a)]
[1]*Harvard University, Cambridge, Massachusetts 02138, USA*
[2]*IBM T. J. Watson Research Center, Yorktown Heights, New York 10598, USA*
[3]*Duke University, Durham, North Carolina 27708, USA*

(Received 3 October 2014; accepted 3 November 2014; published online 17 November 2014)

Zinc oxysulfide, Zn(O,S), films grown by atomic layer deposition were incorporated with aluminum to adjust the carrier concentration. The electron carrier concentration increased up to one order of magnitude from 10^{19} to 10^{20} cm^{-3} with aluminum incorporation and sulfur content in the range of $0 \leq S/(Zn+Al) \leq 0.16$. However, the carrier concentration decreased by five orders of magnitude from 10^{19} to 10^{14} cm^{-3} for $S/(Zn+Al) = 0.34$ and decreased even further when $S/(Zn+Al) > 0.34$. Such tunable electrical properties are potentially useful for graded buffer layers in thin-film photovoltaic applications. *© 2014 AIP Publishing LLC*.
[http://dx.doi.org/10.1063/1.4901899]

Zinc oxysulfide, Zn(O,S), has recently been demonstrated as a promising *n*-type material partner for various *p*-type absorber materials, such as $Cu(In,Ga)(S,Se)_2$ (CIGS),[1,2] $Cu_2ZnSn(Se,S)_4$ (CZTS),[3–5] and SnS.[6–9] Compared to the conventional toxic CdS buffer material for CIGS and CZTS solar cells, Zn(O,S) is composed of earth-abundant and non-toxic elements. This ternary *n*-type buffer material also has the advantage of having the ability to adjust the band alignment through fine tuning of the stoichiometry, which is easily achieved by atomic layer deposition (ALD) through varying the precursor pulse ratios.[10–12] Increasing the sulfur content in Zn(O,S) raises the conduction band energy, which is critical in adjusting the conduction band offset (CBO) at the buffer/absorber interface to optimize the solar cell device performance,[13] as illustrated for SnS/Zn(O,S) heterojunctions in Fig. S1 (see Ref. 14). If the conduction band energy of the buffer layer is too low compared to that of the absorber layer, the negative CBO will induce recombination at the buffer/absorber interface via defects (Fig. S1(a)).[15] If the conduction band energy of the buffer layer is too high compared to that of the absorber layer, the positive CBO at the buffer/absorber interface creates a barrier that prevents electrons from flowing across the junction towards the transparent conducting oxide (TCO) layer (Fig. S1(b)).

In addition to fine tuning of the band alignment through varying the stoichiometry of Zn(O,S), tuning of the electrical properties of Zn(O,S) can significantly influence the solar cell device performance. In recent studies[16] of SnS-based solar cells, during the process of optimizing the Zn(O,S) stoichiometry, the oxygen content of Zn(O,S) was increased to lower the CBO at the SnS/Zn(O,S) interface. However, this resulted in ohmic behavior of the solar cell device due to the increased conductivity of Zn(O,S). The rectifying behavior of SnS-based solar cells was recovered and higher efficiencies were achieved through nitrogen doping of the Zn(O,S) buffer layer, which reduced the electron carrier concentration of Zn(O,S).[16] Reduction in electron carrier concentration of Zn(O,S) can also be achieved through post-deposition annealing in oxygen, and the extent of carrier density reduction can be varied depending on the annealing temperature and the sulfur content in Zn(O,S).[17]

Although it has been demonstrated that low electron carrier concentration of Zn(O,S) can improve SnS-based solar cells, this can increase contact resistance with the TCO layer by adding series resistance to the solar cell, which reduces the short-circuit current density (J_{SC}). While a low carrier concentration of Zn(O,S) can be beneficial for the portion of the buffer layer closer to the absorber layer to reduce possible recombination occurring at the absorber/buffer interface, a high carrier concentration of Zn(O,S) can be beneficial for the portion of the buffer layer closer to the TCO layer to reduce contact resistance. Aluminum is a well known dopant for increasing the electron carrier concentration of ZnO for TCO applications.[18,19] In this study, we report that the electron carrier concentration of ALD Zn(O,S) can be either increased or decreased by modifying the stoichiometry of the film with aluminum incorporation, which is potentially useful for graded buffer layers in thin-film solar cell applications.

A custom-built hot-wall ALD reactor was used to grow Zn(O,S) and Al-incorporated Zn(O,S) films. Films were grown at a deposition temperature of 120 °C in closed valve mode. The precursors used were diethylzinc (DEZ, $Zn(C_2H_5)_2$), deionized H_2O, a gas mixture of 4% H_2S in N_2, and trimethylaluminum (TMA, $Al(CH_3)_3$) for the zinc, oxygen, sulfur, and aluminum sources, respectively. Purified N_2 was used as the purging gas. All of the precursors were kept at room temperature. The exposures used for each dose of DEZ, H_2O, H_2S, and TMA are estimated to be approximately 0.13, 0.15, 6.50, and 0.22 Torr·s, respectively. The ALD sequence for Zn(O,S) was $(DEZ/N_2/H_2O/N_2) \times m + (DEZ/N_2/H_2S/N_2) \times 1$, where the stoichiometry was varied by tailoring *m* for different sulfur incorporation into the films. The ALD sequence for Al-incorporated Zn(O,S) was

a)Electronic mail: gordon@chemistry.harvard.edu

 © 2014 AIP Publishing LLC

This article is copyrighted as indicated in the article. Reuse of AIP content is subject to the terms at: http://scitation.aip.org/termsconditions. Downloaded to IP: 66.31.20.16 On: Wed, 19 Nov 2014 17:47:27

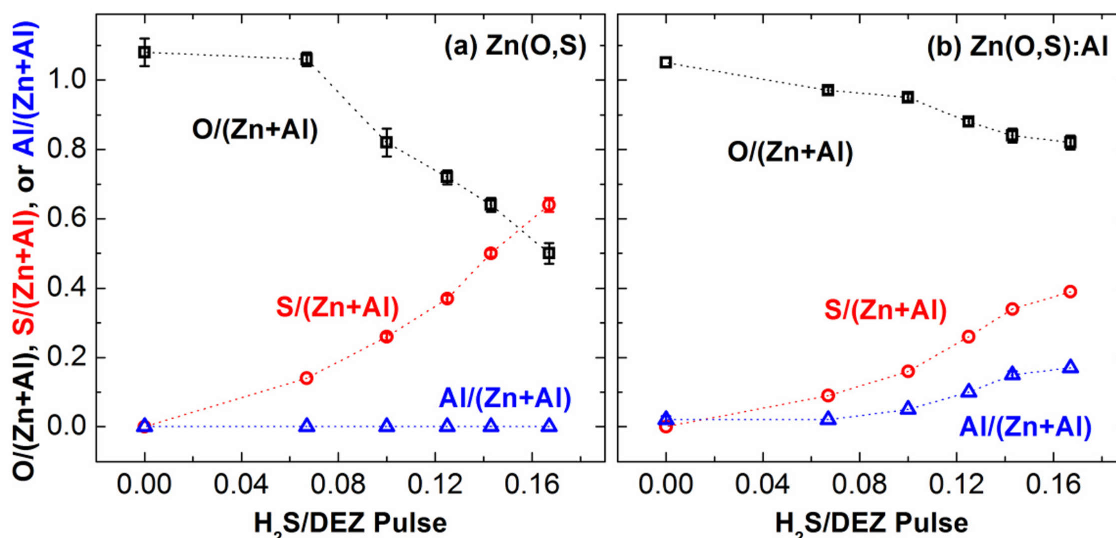

FIG. 1. Plots of O/(Zn+Al) (black), S/(Zn+Al) (red), and Al/(Zn+Al) (blue) vs. (the number of H_2S pulses)/(the number of DEZ pulses) for Zn(O,S) films (a) without and (b) with Al incorporation.

($DEZ/N_2/H_2O/N_2$) $\times$ m + ($DEZ/N_2/H_2S/N_2$) $\times$ 1 + ($DEZ/N_2/H_2O/N_2$) $\times$ (m–1) + ($DEZ/N_2/TMA/N_2/H_2O/N_2$) $\times$ 1 + ($DEZ/N_2/H_2S/N_2$) $\times$ 1, where aluminum was incorporated into every other Zn(O,S) ALD cycle.

Stoichiometry of the films was measured by Rutherford backscattering spectroscopy (RBS). The carrier type and carrier density were determined by van der Pauw and Hall effect measurements on 5 mm $\times$ 5 mm samples with films approximately 250 nm thick. The carrier mobility was then determined assuming a single carrier type using: $\rho = 1/ne\mu$, where ρ is the resistivity, n is the carrier density, e is the electron charge, and μ is the carrier mobility. Very resistive ($\rho > 100\ \Omega\cdot$cm) or low mobility ($\mu < 10\,\text{cm}^2/\text{V}\cdot\text{s}$) samples were measured by a rotating magnet Hall measurement system, which uses a lock-in detection technique to extract the Hall signal with better sensitivity.[20] The crystal structure and texture of the films were analyzed by x-ray diffraction (XRD, PANalytical X-Pert Pro) with Cu $K\alpha$ radiation using θ–2θ scan. The absorption coefficient (α) and optical bandgap (E_g) were determined by measuring the optical transmittance and reflectance spectra from a UV/visible spectrophotometer with an integrating sphere (Hitachi U-4100). Films were grown on glassy carbon substrates for RBS and on quartz substrates for Hall, bandgap measurements, and XRD analysis. It should be noted that the crystallinity of the film may change depending on the substrate,[21] which may also affect the electrical properties of the film. Though the substrates for characterization are different from the actual solar cell applications, the controlled experiments on quartz substrates still give indication of what is occurring in the Zn(O,S) films with aluminum incorporation.

Figure 1 shows the sulfur, oxygen, and aluminum contents as a function of the number of H_2S pulses to the number of DEZ pulses for Zn(O,S) and aluminum-incorporated Zn(O,S) films, determined by RBS. The

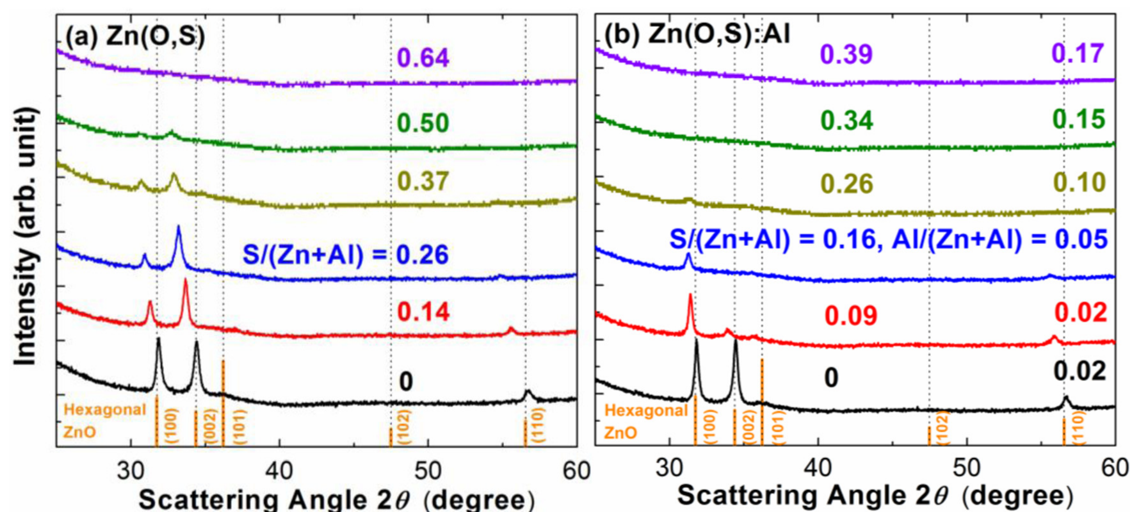

FIG. 2. X-ray diffraction of Zn(O,S) films (a) without and (b) with Al incorporation for various S/(Zn+Al) and Al/(Zn+Al) ratios. Vertical lines are for the hexagonal ZnO (JCPDS No. 01-079-2204).

This article is copyrighted as indicated in the article. Reuse of AIP content is subject to the terms at: http://scitation.aip.org/termsconditions. Downloaded to IP: 66.31.20.16 On: Wed, 19 Nov 2014 17:47:27

sulfur content in the Zn(O,S) films is higher than the precursor pulse ratio, which has been previously reported.[11] For example, S/(Zn+Al) is 0.26 for Zn(O,S) when the H_2S to DEZ pulse ratio is 0.10. The aluminum content in the aluminum-incorporated Zn(O,S) films increased with the H_2S to DEZ pulse ratio, due to the ALD sequence used to grow these films. Compared to the Zn(O,S) films without aluminum, the aluminum incorporation decreased the sulfur content while it increased the oxygen content in the films, as shown in Fig. 1(b). This effect was enhanced as more aluminum was incorporated into the films, indicating that the aluminum is inhibiting sulfur and promoting oxygen incorporation.

X-ray diffraction scans of films with and without aluminum incorporation with different sulfur and aluminum contents are shown in Fig. 2. With increasing sulfur in the films, the peaks shifted towards lower scattering angles indicating increasing lattice constants due to the substitution of larger sulfur for smaller oxygen.[11,17] Preferred crystal orientation of the films also changed with aluminum incorporation. The hexagonal ZnO (002) peaks were highest in intensity for Zn(O,S) films without aluminum, whereas the (100) peaks were highest for the Zn(O,S) films with aluminum. For both films with and without aluminum, the amplitudes of the diffraction peaks decreased with increasing sulfur content due to an increase of an amorphous or nano-crystalline component of the films. The diffraction peaks disappeared when $S/(Zn+Al) \geq 0.64$ for the films without aluminum indicating nano-crystalline or amorphous films. The diffraction peaks started to disappear at lower sulfur contents in the aluminum-incorporated films compared to the films without aluminum. No diffraction peaks were detected for $S/(Zn+Al) \geq 0.34$ for the aluminum-incorporated films.

The resistivity, electron carrier concentration, and carrier mobility are plotted as a function of the S/(Zn+Al) ratio for Zn(O,S) films with and without aluminum, as shown in Fig. 3. For the Zn(O,S) films without Al, the carrier mobility decreased steadily with increasing sulfur content due to the increased disorder in the anion sublattice. The electron carrier concentration remained on the order of 10^{19} cm^{-3} as previously reported.[17] For the Al-incorporated Zn(O,S) films, the electron carrier concentration increased by up to an order of magnitude from 10^{19} to 10^{20} cm^{-3} for low sulfur contents ($0 \leq S/(Zn+Al) \leq 0.16$), due to the expected Al substitution for Zn. But for somewhat higher sulfur contents ($0.34 \leq S/(Zn+Al) \leq 0.39$), Al incorporation surprisingly decreased the electron carrier concentration by about five orders of magnitude from 10^{19} to 10^{14} cm^{-3}. For the films with the highest sulfur contents ($S/(Zn+Al) = 0.48$ and 0.55), the weak Hall signal remained the same polarity when applying both positive and negative magnetic fields, which may be due to having comparably low concentrations of both electrons and holes. Such an abrupt decrease in carrier concentration may be due to precipitation of an insulating nanoscale aluminum-oxide phase, which is correlated with the increased aluminum and oxygen incorporation (Fig. 1).

The aluminum-incorporated films overall showed lower carrier mobility than the films without Al due to increased disorder introduced to the films by the aluminum, as evidenced by the XRD scans (Fig. 2). The carrier mobility of

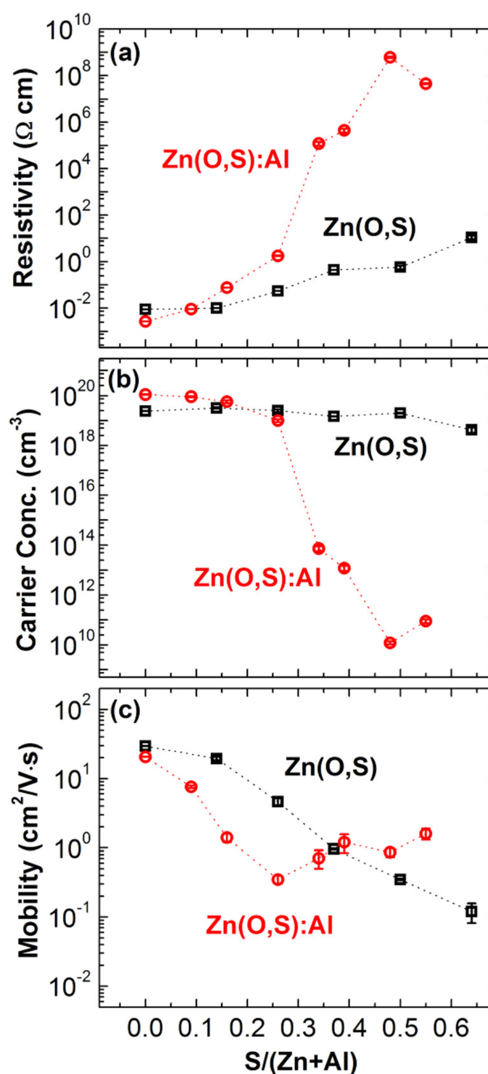

FIG. 3. Plots of (a) resistivity, (b) electron carrier concentration, and (c) carrier mobility vs. S/(Zn+Al) for Zn(O,S) (black) and Zn(O,S):Al (red) films.

the aluminum-incorporated Zn(O,S) films also initially decreased with increasing sulfur content for $S/(Zn+Al) \leq 0.26$ due to the increased disorder in the anion sublattice. Then, the mobility increased with increasing sulfur content when $S/(Zn+Al) \geq 0.34$, while the carrier concentration decreased further. Lowered carrier concentration typically results in higher mobility, but these carrier concentrations are too small to explain this trend.

From plots of α^2 vs. photon energy for Zn(O,S) and Zn(O,S):Al films with various stoichiometries, as shown in Fig. S2 (see Ref. 14), Tauc's relation for direct transitions was used to determine the optical bandgap energy values[22]

$$\alpha(h\nu) \propto (h\nu - E_g)^{1/2}, \quad (1)$$

where $\alpha(h\nu)$ is the absorption coefficient, $h\nu$ is the photon energy, and E_g is the optical bandgap. The electron and hole effective masses are assumed to be constant. Bandgap energy values are plotted as a function of sulfur concentration for Zn(O,S) films with and without Al, as shown in Fig. 4. Aluminum incorporation increased the bandgap values of the films. Formation of amorphous $ZnAl_xO_y$ or Al_2O_3 with much

This article is copyrighted as indicated in the article. Reuse of AIP content is subject to the terms at: http://scitation.aip.org/termsconditions. Downloaded to IP: 66.31.20.16 On: Wed, 19 Nov 2014 17:47:27

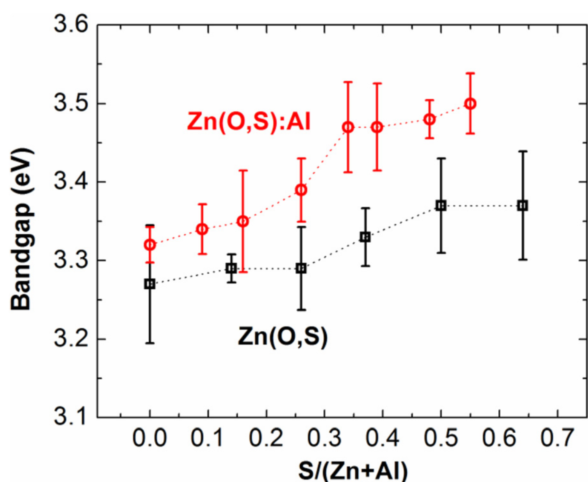

FIG. 4. Bandgap, determined from absorption data, vs. S/(Zn+Al) for Zn(O,S) (black) and Zn(O,S):Al (red) films.

higher bandgaps could contribute to the increase in bandgap with aluminum incorporation. The Burstein-Moss effect[23] might contribute to the increase in optical bandgap energy for $0 \leq$ S/(Zn+Al) ≤ 0.16 where the carrier concentrations are at degenerate levels ($>10^{19}$ cm^{-3}). In this range, the Al-incorporated films have high electron carrier concentrations (Fig. 3(b)), which increase the Fermi level in the conduction band. However, for Al-incorporated Zn(O,S) films with S/(Zn+Al) ≥ 0.34, the optical bandgap energies increase further despite the significant decrease in electron carrier concentration (Fig. 3(b)). Thus, the Burstein-Moss effect does not explain the wider bandgaps in the aluminum-incorporated sulfur-rich films.

In summary, it was demonstrated that Zn(O,S) can be incorporated with aluminum to either increase or decrease the carrier concentration depending on the stoichiometry of the films. When $0 \leq$ S/(Zn+Al) ≤ 0.16, electron carrier concentration was increased up to the order of 10^{20} cm^{-3} and carrier mobility decreased with increasing sulfur in the Al-incorporated Zn(O,S) films. On the other hand, when S/(Zn+Al) ≥ 0.34, carrier concentration was decreased at least by five orders of magnitude to the order of 10^{14} cm^{-3} and mobility increased with increasing sulfur in the Al-incorporated films. Such tunable properties can potentially improve photovoltaic (PV) device performance through electrically graded Zn(O,S) buffer layers in combination with compatible absorber materials.

The work presented herein was funded in part by an agency of the United States Government; see the supplementary material section of this article for more information.[14]

The authors thank Professor Eric Mazur for access to the Hall system and the UV/visible spectrophotometer. This material is based upon work supported by the U.S. Department of Energy, Energy Efficiency and Renewable Energy Program, under Award No. DE-EE0006334. Part of the work was performed at the Center of Nanoscale Systems (CNS) at Harvard University, a member of the National Nanotechnology Infrastructure Network (NNIN), which is supported by NSF (ECS-0335765).

[1]A. Hultqvist, C. Platzer-Bjorkman, E. Coronel, and M. Edoff, Sol. Energy Mater. Sol. Cells **95**, 497–503 (2011).
[2]I. Repins, M. A. Contreras, B. Egaas, C. DeHart, J. Scharf, C. L. Perkins, B. To, and R. Noufi, Prog. Photovoltaics **16**, 235–239 (2008).
[3]B. Shin, O. Gunawan, Y. Zhu, N. A. Bojarczuk, S. J. Chey, and S. Guha, Prog. Photovoltaics **21**, 72–76 (2013).
[4]W. Wang, M. T. Winkler, O. Gunawan, T. Gokmen, T. K. Todorov, Y. Zhu, and D. B. Mitzi, Adv. Energy Mater. **4**, 1301465 (2014).
[5]D. A. R. Barkhouse, R. Haight, N. Sakai, H. Hiroi, H. Sugimoto, and D. B. Mitzi, Appl. Phys. Lett. **100**, 193904 (2012).
[6]K. Hartman, J. L. Johnson, M. I. Bertoni, D. Recht, M. J. Aziz, M. A. Scarpulla, and T. Buonassisi, Thin Solid Films **519**, 7421–7424 (2011).
[7]P. Sinsermsuksakul, K. Hartman, S. B. Kim, J. Heo, L. Z. Sun, H. H. Park, R. Chakraborty, T. Buonassisi, and R. G. Gordon, Appl. Phys. Lett. **102**, 053901 (2013).
[8]H. H. Park, R. Heasley, L. Sun, V. Steinmann, R. Jaramillo, K. Hartman, R. Chakraborty, P. Sinsermsuksakul, D. Chua, T. Buonassisi, and R. G. Gordon, "Co-optimization of SnS absorber and Zn(O,S) buffer materials for improved solar cells," Prog. Photovoltaics (published online).
[9]V. Steinmann, R. Jaramillo, K. Hartman, R. Chakraborty, R. E. Brandt, J. R. Poindexter, Y. S. Lee, L. Sun, A. Polizzotti, H. H. Park, R. G. Gordon, and T. Buonassisi, "3.88% efficient tin sulfide solar cells using congruent thermal evaporation," Adv. Mater. (published online).
[10]J. R. Bakke, J. T. Tanskanen, C. Hagglund, T. A. Pakkanen, and S. F. Bent, J. Vac. Sci. Technol., A **30**, 01A135 (2012).
[11]C. Platzer-Björkman, T. Törndahl, D. Abou-Ras, J. Malmström, J. Kessler, and L. Stolt, J. Appl. Phys. **100**, 044506 (2006).
[12]T. J. Larrabee, T. E. Mallouk, and D. L. Allara, Rev. Sci. Instrum. **84**, 014102 (2013).
[13]L. Sun, R. Haight, P. Sinsermsuksakul, S. B. Kim, H. H. Park, and R. G. Gordon, Appl. Phys. Lett. **103**, 181904 (2013).
[14]See supplementary material at http://dx.doi.org/10.1063/1.4901899 for the supplementary figures (S1 and S2).
[15]T. Minemoto, T. Matsui, H. Takakura, Y. Hamakawa, T. Negami, Y. Hashimoto, T. Uenoyama, and M. Kitagawa, Sol. Energy Mater. Sol. Cells **67**, 83 (2001).
[16]P. Sinsermsuksakul, L. Sun, S. W. Lee, H. H. Park, S. B. Kim, C. Yang, and R. G. Gordon, Adv. Energy Mater. **4**, 1400496 (2014).
[17]H. H. Park, R. Heasley, and R. G. Gordon, Appl. Phys. Lett. **102**, 132110 (2013).
[18]Y. Kim, W. Lee, D. R. Jung, J. Kim, S. Nam, H. Kim, and B. Park, Appl. Phys. Lett. **96**, 171902 (2010).
[19]J. I. Kim, W. Lee, T. Hwang, J. Kim, S. Lee, S. Kang, H. Choi, S. Hong, H. H. Park, T. Moon, and B. Park, Sol. Energy Mater. Sol. Cells **122**, 282 (2014).
[20]O. Gunawan and T. Gokmen, "Hall measurement system with rotary magnet," U.S. patent application US20140028306 (2014).
[21]T. Wada, Sol. Energy Mater. Sol. Cells **49**, 249 (1997).
[22]J. Tauc, Mater. Res. Bull. **5**, 721 (1970).
[23]E. Burstein, Phys. Rev. **93**, 632 (1954).

This article is copyrighted as indicated in the article. Reuse of AIP content is subject to the terms at: http://scitation.aip.org/termsconditions. Downloaded to IP: 66.31.20.16 On: Wed, 19 Nov 2014 17:47:27